

# OPTICAL DIAGNOSTICS OF THE CYCLE-TO-CYCLE VARIATION IN THE KERNEL DEVELOPMENT AND ABNORMAL COMBUSTION: SI SMALL ENGINE

**Rémi Ballais**

*SUPMÉCA/LISMMA-Paris, School of Mechanical and Manufacturing Engineering  
3 rue Fernand Hainaut - 93407 Saint-Ouen Cedex, France  
e-mail: remi.ballais@supmeca.fr*

**Jose Manuel Gallardo-Ruiz**

*E.T.S. Ingenieros Industriales, University of Malaga  
Dr. Ortiz Ramos s/n, 29071 Málaga, Spain  
e-mail: josemgallardo@uma.es*

**Simona Silvia Merola, Paolo Sementa, Cinzia Tornatore**

*Istituto Motori – CNR  
via G. Marconi, 8 – 80125 Napoli (Italy)  
emails: s.merola@im.cnr.it, p.sementa@im.cnr.it, c.tornatore@im.cnr.it*

## **Abstract**

*The combustion stability and more in details the cyclic variability significantly influences the performance and the pollutant emissions of a spark ignition engine. In this work, an experimental research activity was carried out to investigate the influence of the different combustion phases on the cycle-to-cycle variation. In particular the flame kernel development and the fuel deposits burning were investigated by in-cylinder pressure measurements and optical investigations. Engine cycle resolved visualization was applied to characterize the spatial evolution of the flame front from the spark ignition until the exhaust phase. A numerical custom post-detection procedure was used to correlate the optical data with the pressure related parameters during the combustion process. The simultaneous use of optical diagnostics and pressure related analysis demonstrated the fundamental role of the first stage and late phase of the combustion on the spark ignition engine process. Flame kernel and diffusion controlled flame due to fuel deposits burning dominated the cyclic variability of in-cylinder combustion. The experiments were realized in a 250 cm<sup>3</sup> single cylinder, port fuel injection, four-stroke spark ignition engine. The engine was optically accessible and it was equipped with the head, injection system and exhaust device of a commercial engine mounted on small motorcycles and scooters. Standard EURO IV gasoline was used.*

**Keywords:** *optical diagnostics; cycle-to-cycle variation; flame kernel; abnormal combustion; SI engine*

## **1. Introduction**

Nowadays, spark ignition engines equip the most part of two and four wheels vehicles in the urban areas. The almost totality of these engines are ported fuel injection. The automotive world is strongly influenced by energy, environmental and market needs. Thus it is oriented towards SI small engines with high-performance, reduced fuel consumption and environmental impact. Since a long time, the cycle-to-cycle variation has been known to have a significant effect on engine efficiency [1]. It is generally caused by variations of the in-cylinder fuel-air mixture, the spark discharge characteristics, level of turbulences or the air flow features [2]. Despite the high technological innovation of SI engines, a further optimization is still possible for the small engines in particular at low engine speed and high load, which were shown as unstable operating conditions. The fuel

storage on the port and on the intake valves puddles determines variations of the air/fuel ratio that influences the combustion process, the pollutant formation and the effectiveness of post treatment devices, eventually present. The study was aimed to improve the basic knowledge about the physical and chemical processes that take place in a PFI SI small engine. The overall combustion process, from the spark ignition to the late combustion phase, was followed using cycle resolved visualization. Thus, it was possible to study of the cycle-to-cycle variation taking advantage of the synergy offered by the coupling of optical diagnostics and pressure related parameters acquisition.

## 2. Experimental apparatus

The experimental investigations were performed on an optically accessible single-cylinder, PFI, four-stroke SI engine. The engine bore and stroke were 72 mm and 60 mm, respectively, and the geometric compression ratio was 10. The optical engine was equipped with the cylinder head of a commercial 250 cc motorcycles engine with four valves and pent-roof geometry. The spark plug was centrally located and a quartz pressure transducer was flush-installed between the exhaust and inlet valves in the combustion chamber to acquire the pressure signal without changing the original compression ratio. The in-cylinder pressure, the rate of chemical energy release and the related parameters were evaluated on an individual cycle basis or averaged on 400 cycles [1]. A lambda sensor was set up at the engine exhaust to measure the air/fuel ratio.

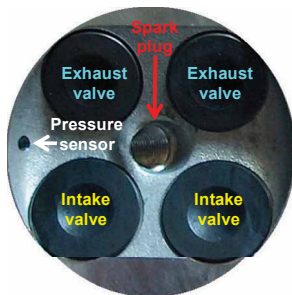


Fig. 1. View of the head from the bottom

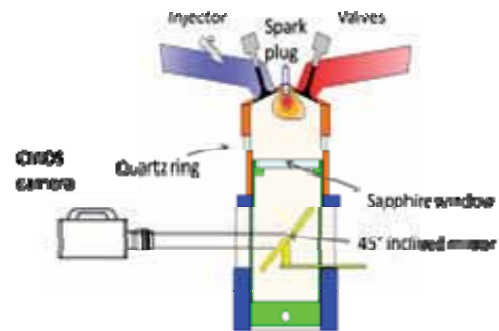


Fig. 2. Workbench scheme

The piston employed was specially manufactured for optical diagnostics. It was an elongated piston and its crown was replaced by a 58.5 mm bore transparent sapphire window. Self-lubricating Teflon-bronze composite piston rings were used to avoid the oil deposits in the optical section. The lube oil and coolant conditioning unit used were special customized for transparent single cylinder engine application. To heat up the engine as well as the engine lube oil, a coolant heater was installed in the cooling water circuit and exchanged the heat via the coolant/oil heat exchanger. Cycle resolved flame visualization was performed using an 8-bit high speed CMOS (complementary metal-oxide semiconductor) camera. The camera mounted a 50 mm focal Nikon lens. The detection speed was 5000 fps for 512x512 pixel full chip and the spectral range extended from 380 nm to 780 nm. A camera region of interest was selected (360 x 360 pixel) to obtain the best match between spatial and temporal resolution. This optical assessment allowed a spatial resolution around 0.22 mm/pixel and a frame rate of 7188 fps. The exposure time was fixed at 10  $\mu$ s which corresponds to 0.18° CA. A 45° UV-Visible mirror was placed at the bottom of the engine to reflect the luminosity signal from the combustion chamber to the CMOS camera. The Crank Angle Encoder signal synchronized the camera and the engine through a unit delay. AVL Indimodul recorded the TTL signal from the camera acquisitions together with the signal acquired by the pressure transducer. In this way, it was possible to determine the crank angles where optical data were detected. It recorded also the signals from all the sensors (Lambda sensor, pressure transducer...) and calculated the values pressure derived parameters as, for example, the Rate of

Heat Release. The 3 holes original injector was used for the tests. The injection of the fuel started at 245°CA ATDC and lasted 175 °CA, the amount injected provided a stoichiometric air/fuel ratio in the combustion chamber. The fuel was injected in the intake manifold when the inlet valves were open. The throttle was wide open and the spark timing was fixed at 22°CA BTDC, in order to reach the maximum brake torque avoiding the knocking. The engine was fueled with a commercial EURO 4 gasoline. All the measurements were performed at an engine speed of 3000 rpm.

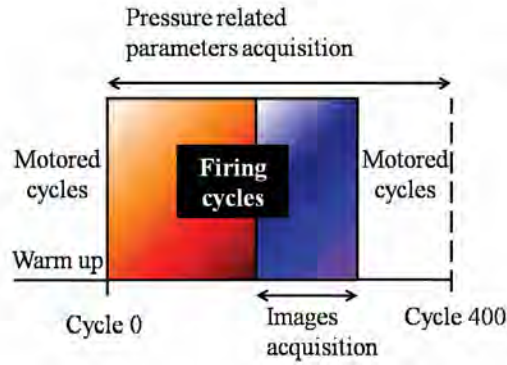


Fig. 3. Sketch of the test procedure

The acquisitions started after a warm-up phase. During this phase, an electric engine drives the optical one. The warm up interrupted when the desired temperature of 60° was reached in the cooling system to simulate real working conditions. The tests were carried out during a number of 400 cycles in order to have a good statistics without wearing the piston rings. The images were acquired during about 25 cycles. Then the engine returned in motored condition for a few cycles (Fig. 3). This phase allowed checking an eventual change in the thermal and fluid-dynamic status of the engine from the beginning of the measurements. The pressure data were post-processed using a numerical procedure developed in LabView of National Instruments environment. The procedure evaluated the maximum pressure value and the related CAD for each engine cycle. Same procedure was applied for the heat release values. A retrieving procedure of the optical data was realized to process each image. The optical diagnostics consisted in capturing and post-processing the global luminosity emitted in the combustion chamber in the visible range. The external spurious light determined some interferences and ghosts that influenced the image quality. The spurious light was reflected on the piston skirt creating on the images a luminous annulus around the limits of the combustion chamber. In order to eliminate these interferences, a reference image was used as background and then it was subtracted from the analyzed images. After this step a region of interest was selected. This operation allowed eliminating the luminous noise due to the reflections of the combustion process radiative emission on the piston wall. The reference image was detected at the CAD before the spark ignition timing for each engine cycle. Each image was converted in a numerical matrix. The global luminosity was calculated by the integration of luminosity from each pixel. The mean integral signals were evaluated dividing the total intensity by the pixel number in the selected region of interest. Thus the intensities resulted in 8-bit scale. This procedure allowed comparing different cycles and experiments without the influence of the optical setup parameters (exposure time, gate etc...). The luminous signals and the pressure related values were correlated following a statistical approach. The Coefficient of Variation COV and Coefficient Of Correlation R was calculated according to the relations:

$$R(X, Y) = \frac{Co\ var(X, Y)}{V(X)V(Y)}, \text{ where } Co\ var(X, Y) = \sum_1^n \frac{(X_i - \bar{X})(Y_i - \bar{Y})}{n - 1}, \ COV(X) = \frac{\bar{X}}{V(X)} * 100, \quad (1)$$

$\bar{X}$  : mean value of X,  $\bar{Y}$  : mean value of Y and  $V(X)$  is the standard deviation of X.

For optical and pressure data the COV at maximum values was calculated. The COV at the pressure peak is a standard parameter to estimate the engine cycle variability. This value is suitable for the quick evaluation of the engine combustion efficiency; on the other hand it is not enough to understand the complex phenomena correlated to the overall combustion process. To better investigate these phenomena, the COVs were also evaluated from the spark timing until the opening of the exhaust valves for all the optical and pressure data.

### 3. Results and discussion

Figure 4 reports the flame propagation detected in the combustion chamber for a selected engine cycle. The evidence of spark ignition occurred around  $22^\circ$  BTDC and it was represented by a luminous arc near the spark plug. Spark plasma emission persisted for about 2-3 CAD. Then the flame kernel was observable, even if its luminosity was very lower than the spark. Then the flame kernel was well resolvable and it moved from the spark plug towards the cylinder walls with a radial like behaviour (images 1-2). Then, an asymmetry with some negative curvatures in the flame front shape was noticed. The flame front goes faster near the exhaust valves part reaching the walls just around 2 CAD BTDC (images 3-6). Moreover, several bright spots were detected in the burned gas before the flame front reached the chamber walls. These phenomena were due to the presence of liquid fuel in the combustion chamber. It is known that in a PFI engine a part of the injected fuel is deposited on the intake manifold surfaces and forms a layer of liquid film on the valve and port surfaces [3, 4]. The film needs to be re-atomized by the shearing airflow as the intake valves open. If these fuel layers are not well atomized they enter the cylinder as drops and ligaments [5-7]. The fuel deposits were drawn by gravity on the valve head where they remained as film due to the surface tension.

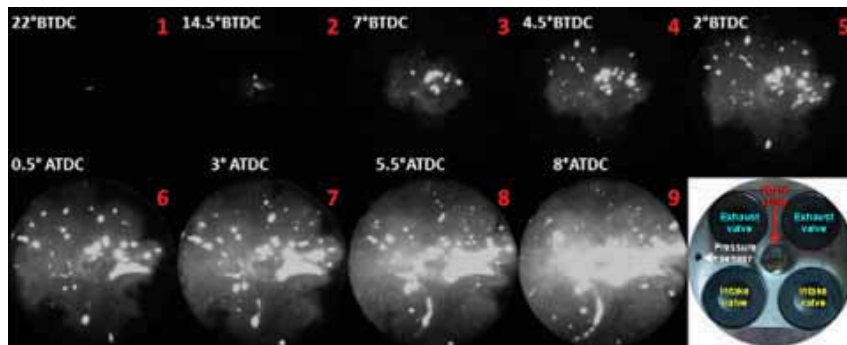


Fig. 4. Cycle-resolved visualization from the spark ignition evidence to the match of the flame front with the combustion chamber walls

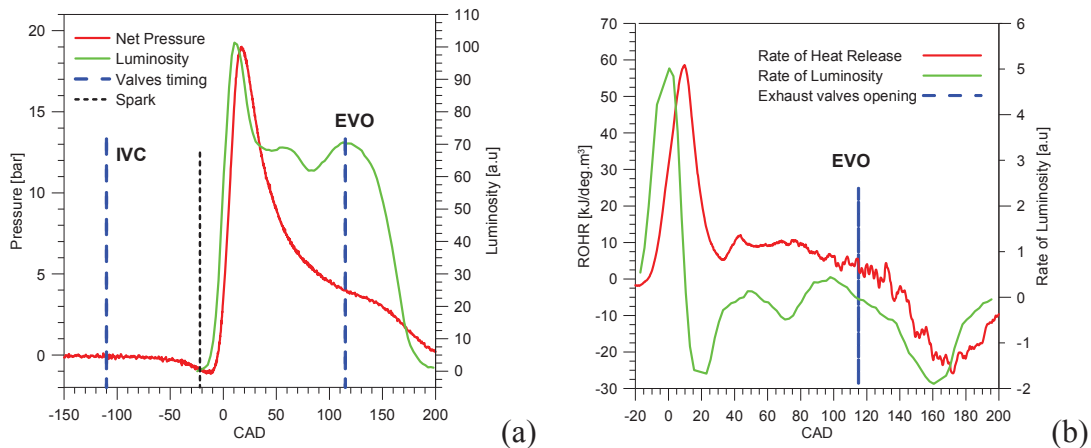
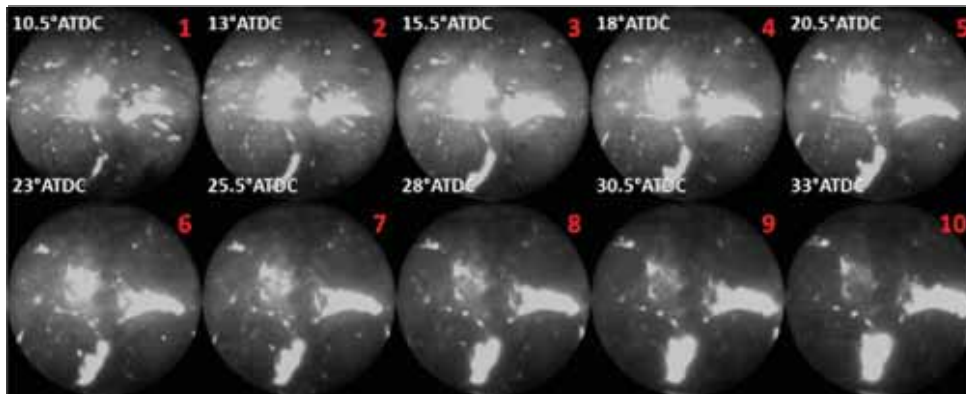
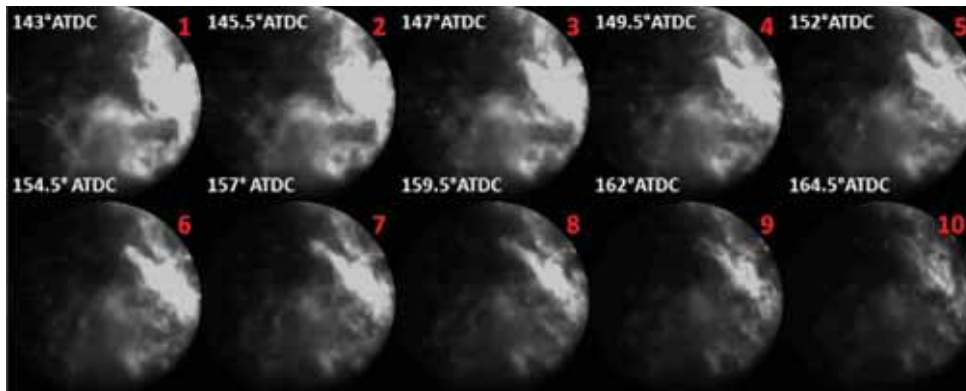


Fig. 5. Comparison between the combustion pressure signal and the integral luminosity (a) and comparison between the rate of heat release and of the integral luminosity (b)

Thus the flame front asymmetry was due to the fuel deposits on the intake valves. When the flame propagates in the normal direction to an area with equivalence ratio gradient, each part of the front evolves in a field with varying fuel concentration. This induces variation of the propagation speed along the flame front and an increase in flame wrinkling. Moreover, since the injection occurred in the open valves state, part of the injected fuel droplets was directly carried into the combustion chamber due to the gas flow. The droplets stuck on the cylinder walls and the piston surface. These fuel deposits created fuel-rich zones with sub-millimetre size that ignited when reached by the normal flame front causing the bright spots. The presence of fuel deposits as squeezed film or impinged droplets had direct effect on flame radius evolution in terms of kernel cyclic variability and flame stability [8, 9]. The pressure signal after the subtraction of the motored one was considered for each engine cycle and compared with the integral luminosity measured by CMOS detection in the combustion chamber. Moreover a comparison between the rate of heat release and of the integral luminosity was performed too. The results obtained for the engine cycle of Fig. 4 are shown in Fig. 5. From the spark ignition to the maximum values (near 15° ATDC) the luminous and pressure signals showed the same trend (Fig. 5a). This was due to the chemical reactions which occurred in the first times of the combustion process that are exothermic and radiative and that promote the increasing of the pressure. In fact, in the early stages of the in-cylinder combustion, the chamber volume was still small and the flame front speed was high enough to release a sufficient amount of heat to make the pressure rising up (the ROHR reaches its maximum near the peak of pressure regarding the Fig. 5b).



*Fig. 6. Cycle-resolved visualization of combustion phase*



*Fig. 7. Cycle-resolved visualization of late combustion phase*

After 15° ATDC, the combustion pressure and luminous intensity decreased for about 20 CAD. Around 35° ATDC a new increase in the luminosity was detected. This was due to the fuel deposits burning in the intake valves region. In fact, as previously discussed, the port fuel injection created fuel-rich deposits near the intake valves that ignited when the normal flame front reached

them [10, 11]. This incepted diffusion-controlled flames with a strong intensity as shown in Fig. 6. The outlines of the valves are clearly distinguished during the burning of the fuel. Due to the turbulences, the diffusive flames move in the combustion chamber towards the exhaust valves. The diffusion-controlled flames persisted well after the normal combustion event and they are still detectable at the Exhaust Valves Opening (EVO) (Fig. 7). These flames did not contribute to the engine work and then did not influence the pressure signal in agreement with literature [4, 12]. Indeed, the heat released by the chemical reactions during these phenomena is not strong enough to affect the pressure because it is coupled with a high instantaneous volume of the combustion chamber (phase of expansion, ROHR less than 10 kJ/deg·m<sup>3</sup> in this phase according the Fig. 5.b). The initial stages of combustion play an important role on the later flame development [13-15], thus small differences at the kernel formation may produce significant in-cylinder combustion efficiency variations. As a consequence, a correlation between kernel development and cyclic variability subsists. Fig. 8 shows flame images measured at 2.0 CAD BTDC on 10 of 25 consecutive cycles. At this time, the flame kernel was formed and the circular shape of the flame outline can be observed. The bright spots due to the burning of the fuel deposits on the piston surfaces were detected for each cycle. The cyclic variation of the flame is evident.

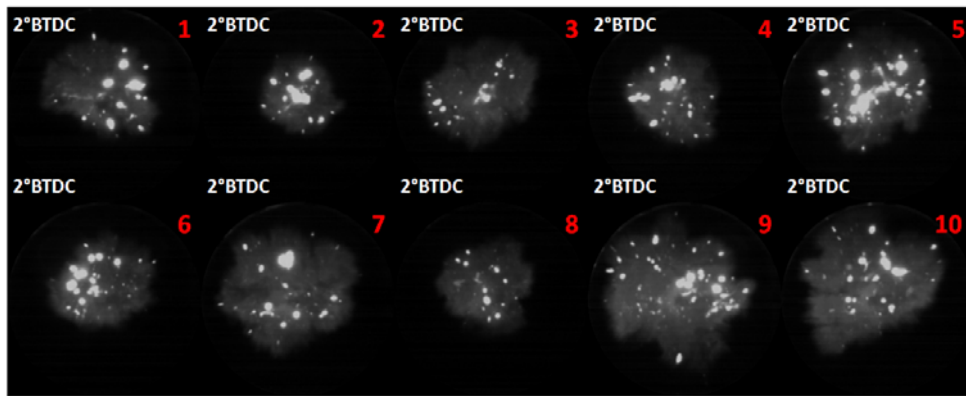


Fig. 8. Flame kernel detected on 10 consecutive cycles at 2.0 CAD BTDC

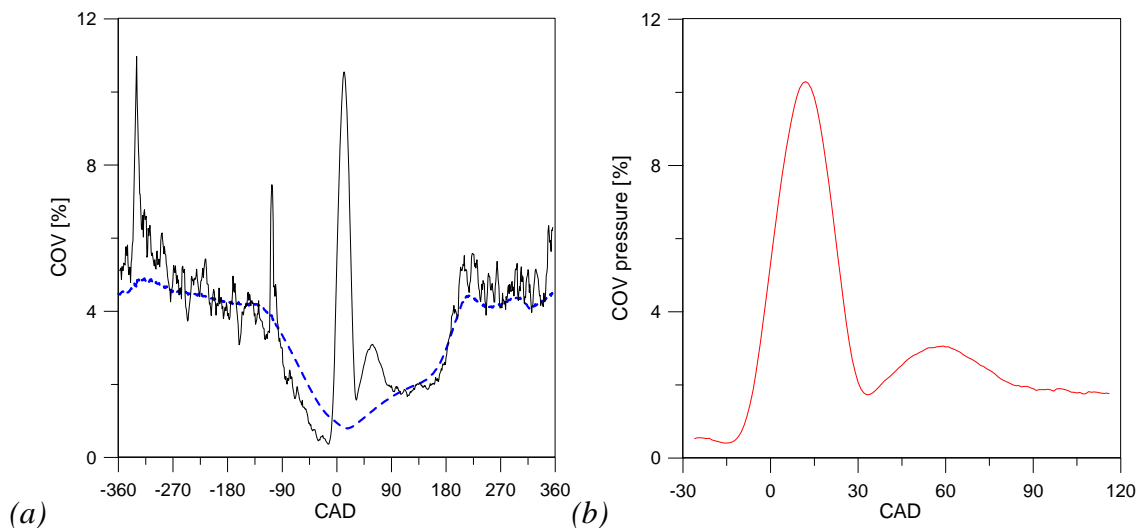


Fig. 9. COV of the in-cylinder pressure. Entire curve (a) and zoom (bt) in the 30°BTDC-120°ATDC range

Conventional analysis of pressure signals allowed to evaluate a COV from pressure peak equal to 9.3% with a correlation coefficient  $R^2=0.83$ . Fig. 9 presents the crank angle resolved COV of the in-cylinder pressure, with an explosion in 30 CAD BTDC-120 CAD ATDC range. From 360 CAD BTDC up to 120 CAD BTDC, the COV shows a weak decreasing on which two spikes are

superimposed. These spikes are due to the intake valve opening and closing, respectively. The COV values are fairly high due to noise that has a relevant weight if compared to the low in-cylinder pressure. After the intake valve closing, the COV reaches a first minimum value. In agreement with literature [15], until the minimum, the COV depends only on the average pressure according the relation:  $COV = \alpha/P^{0.5}$  with P the average pressure, and  $\alpha$  a constant. The  $\alpha$  value is a characteristic of the experimental system and it is the same both in the motored and fired conditions. Thus  $\alpha$  returns the noise level of the engine. In this work  $\alpha \cong 4.8$ . The first COV minimum value corresponds to the normal combustion inception. Following the combustion process, the COV increases, this confirms the increasing in the cyclic variation. The COV reaches the maximum value at CAD closed to the maximum of the heat release rate (Fig. 5b). After this time, the weight of the normal combustion becomes progressively less important than the piston motion. As a consequence, the COV decreases until it reaches a second minimum point. This minimum cannot be considered as a marker of the combustion end. This is due to the abnormal combustion caused by the fuel deposits burning phenomena which is very variable. The COV pressure curve follows the abnormal combustion until the piston expansion becomes leading. Then the in-cylinder pressure decreases. Around 160 CAD ATDC the COV sharply increases to a plateau that corresponds to the exhaust phase. In this time, the COV is less influenced by the in-cylinder pressure than the COV before the combustion starting. This occurs because of the in-cylinder pressure is higher than the motored one at the same CADs. COV from luminosity shows a different trend than COV from pressure as reported in Fig. 10. It allows obtaining additional information in comparison to pressure data. COV from luminous signals is strongly influenced by the early stages of the combustion process and by the late ones. It shows a first local maximum at the kernel flame formation.

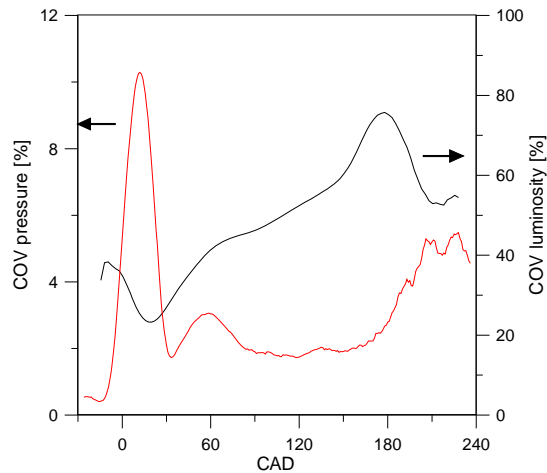


Fig. 10. COV of the in-cylinder pressure and luminosity versus crank angle in the 30 CAD BTDC-360 CAD ATDC range

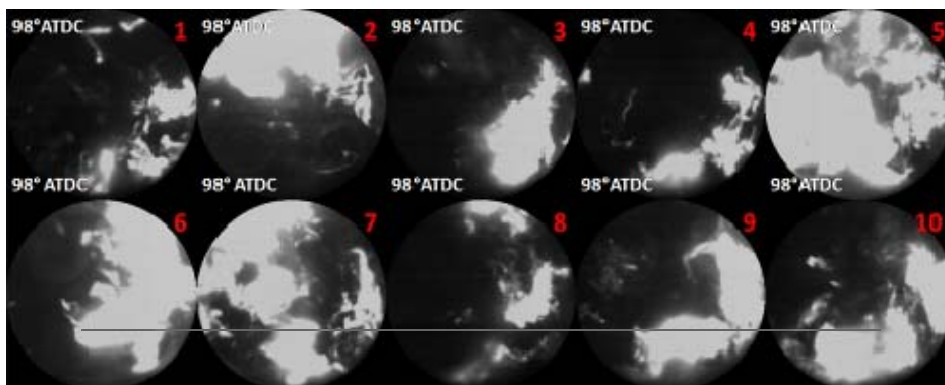


Fig. 11. Cycle-resolved visualization of late combustion phase

This result quantifies the cyclic variability of the kernel. The pressure data analysis does not give the right weight to the early stages of the combustion. As shown in Fig. 8, the flame area in the image 9 is 2.33 bigger than image 8, while the ratio between the related pressures is about 1.006. These instabilities can result negligible if evaluated by the pressure signal. From TDC to 30 CAD ATDC, the spark ignition flame occupies the whole optical section and luminous signal fluctuations are not significant. COV from luminosity reaches a minimum. After the normal combustion event, the inception of the diffusion controlled flames induces a progressive and smooth increasing in the COV from luminous signals.

#### 4. Conclusion

With the aim of optimizing the efficiency of PFI SI small engine, the basic knowledge about the physical and chemical processes needs to be improved. In this work, cycle resolved visualization was applied to characterise the spatial evolution of flame kernel and to follow the flame front propagation in a 250 cm<sup>3</sup> single cylinder, four-stroke PFI SI optically accessible engine. The cycle-to-cycle variation was studied more in details during the early flame development and the late combustion phase. The initial stages of combustion played an important role on the later flame development. Small differences at the kernel formation may produce significant in-cylinder pressure variations. Variations in the fuel-air distribution due to fuel deposits on the intake valves and on the combustion chamber surfaces were proved to be relevant. The simultaneous use of optical diagnostics and pressure related parameters turned out to be relevant to consider the combustion variability through the different combustion phases. In particular, at the first stages of the combustion and during the late phase, the pressure and luminosity COV are very different. Moreover, the level of luminosity COV remains high, it shows that the engine combustion process can be still improved in terms of variability. Thus low cost solutions to improve the PFI SI small engine could be searched for, like changing the injection strategy in terms of duration, start, number of injections.

#### 5. Reference

- [1] Heywood, J. B., *Internal Combustion Engine Fundamentals*, McGraw Hill, 1988.
- [2] Galloni, E., *Analyses about parameters that affect cyclic variation in a spark ignition engine*, Applied Thermal engineering, Vol. 29, pp. 1131-1137, 2009.
- [3] Costanzo, V. S., Heywood, J. B., *Mixture Preparation Mechanisms in a Port Fuel Injected Engine*, SAE Technical Paper n. 2005-01-2080, 2005.
- [4] Nogi, T., Ohyama, Y., Yamauchi, T., Kuroiwa, H., *Mixture Formation of Fuel Injection Systems in Gasoline Engines*, SAE Technical Paper n. 880558, 1988.
- [5] Henein, N. A., Tagomori, M. K., *Cold-start hydrocarbon emissions in port-injected gasoline engines*, Progress in Energy and Combustion Science, Vol. 25, pp. 563-593, 1999.
- [6] Behnia, M., Milton, B. E., *Fundamentals of fuel film formation and motion in SI engine induction systems*, Energy Conversion and Management, Vol. 42, pp. 1751-1768, 2001.
- [7] Gold, M. R., Arcoumanis, C., Whitelaw, J. H., Gaade, J., Wallace, S., *Mixture Preparation Strategies in an Optical Four-Valve Port-Injected Gasoline Engine*, Int. J. of Engine Research, Vol. 1, pp. 41-56, 2000.
- [8] Bianco, Y., Cheng, W., Heywood, J., *The Effects of Initial Flame Kernel conditions on Flame Development in SI Engines*. SAE paper n. 912402, 1992.
- [9] Witze, P., Hall, M., Bennet, M. *Cycle-resolved Measurements of Flame Kernel Growth and Motion Correlated with Combustion Duration*. SAE paper n. 900023, 1990.
- [10] Zhu, G. S., Reitz, R. D., Xin, J., Takabayashi, T. *Modelling Characteristics of Gasoline Wall Films in the Intake Port of Port Fuel Injection Engines*, Int. J. of Engine Research, Vol. 2 (4), pp. 231-248, 2001.

- [11] Merola, S. S., Sementa, P., Tornatore, C., Vaglieco, B. M., '*Effect of Injection Phasing on Valves and Chamber Fuel Deposition Burning in a PFI Boosted Spark-Ignition Engine*', SAE Paper n. 2008-01-0428, 2008.
- [12] Witze, P. O., Green, R. M., '*LIF and Flame-Emission Imaging of Liquid Fuel Films and Pool Fires in an SI Engine During a Simulated Cold Start*' SAE Paper n 970866, 1997.
- [13] Lee, K. H., Kim, K., '*Influence of initial combustion in SI engine on following combustion stage and cycle-by-cycle variations in combustion process*', Int. Journal of Automotive Technology, Vol. 2 (1), pp. 25-31, 2001.
- [14] Mansour, M., Peters, N., Schrader, L. U., '*Experimental study of turbulent flame kernel propagation*' Experimental Thermal and Fluid Science, Vol. 32, pp. 1396-1404, 2008.
- [15] Zervas, E., '*Correlations between cycle-to-cycle variations and combustion parameters of a spark ignition engine*', Applied Thermal Engineering. Vol. 24, pp. 2073-2081, 2004.